SAE TECHNICAL
PAPER SERIES

970630

Comparison Between Air-Assisted and Single-Fluid Pressure Atomizers for Direct-Injection SI Engines Via Spatial and Temporal Mass Flux Measurements

Jeffrey A. Hoffman, Eric Eberhardt, and Jay K. Martin
University of Wisconsin-Madison

SAE The Engineering Society For Advancing Mobility Land Sea Air and Space®
INTERNATIONAL

International Congress & Exposition
Detroit, Michigan
February 24-27, 1997

400 Commonwealth Drive, Warrendale, PA 15096-0001 U.S.A. Tel: (412)776-4841 Fax:(412)776-5760

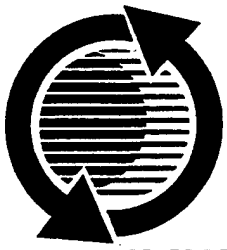

ISSN 0148-7191

Printed in USA

REPORT DOCUMENTATION PAGE

Form Approved
OMB NO. 0704-0188

1. AGENCY USE ONLY *(Leave blank)*	2. REPORT DATE	3. REPORT TYPE AND DATES COVERED
		REPRINT

4. TITLE AND SUBTITLE

TITLE ON REPRINT

5. FUNDING NUMBERS

DAAL03-92-G-0122

6. AUTHOR(S)

AUTHOR(S) ON REPRINT

7. PERFORMING ORGANIZATION NAMES(S) AND ADDRESS(ES)

UNIVERSITY OF WISCONSIN - MADISON
MADISON, WI 53706

8. PERFORMING ORGANIZATION REPORT NUMBER

9. SPONSORING / MONITORING AGENCY NAME(S) AND ADDRESS(ES)

U.S. Army Research Office
P.O. Box 12211
Research Triangle Park,, NC 27709-2211

10. SPONSORING / MONITORING AGENCY REPORT NUMBER

ARO 30340.76-EG-URI

11. SUPPLEMENTARY NOTES

The views, opinions and/or findings contained in this report are those of the author(s) and should not be construed as an official Department of the Army position, policy or decision, unless so designated by other documentation.

12a. DISTRIBUTION / AVAILABILITY STATEMENT

Approved for public release; distribution unlimited.

12 b. DISTRIBUTION CODE

13. ABSTRACT *(Maximum 200 words)*

ABSTRACT ON REPRINT

14. SUBJECT TERMS	15. NUMBER IF PAGES
	16. PRICE CODE

17. SECURITY CLASSIFICATION OR REPORT	18. SECURITY CLASSIFICATION OF THIS PAGE	19. SECURITY CLASSIFICATION OF ABSTRACT	20. LIMITATION OF ABSTRACT
UNCLASSIFIED	UNCLASSIFIED	UNCLASSIFIED	UL

970630

Comparison Between Air-Assisted and Single-Fluid Pressure Atomizers for Direct-Injection SI Engines Via Spatial and Temporal Mass Flux Measurements

Jeffrey A. Hoffman, Eric Eberhardt, and Jay K. Martin
University of Wisconsin-Madison

ABSTRACT

Two distinct atomization strategies are contrasted through the measurement of time and spatially dependent mass flux. The two systems investigated include a pressure atomizer (6.9 MPa opening pressure) and an air-assist atomizer. Both systems have potential for use in direct injection spark ignition engines.

The mass flux data presented were obtained using a spray patternator that was developed to allow phased sampling of the spray. The temporal mass related history of the spray was reconstructed as volume versus time plots and interpolated mass flux contour plots.

Results indicate substantial differences in the distribution of both mass and mass flux in space and time for the two injection systems. For example, the pressure atomizer at high mass delivery rates produced a spray that collapsed into a dispersed cylindrical shape while at low rates, generated a hollow cone structure. In addition, the air-assist device discharges 87% of its injected volume within the first of three poppet oscillations while producing a wide hollow cone structure.

I. INTRODUCTION

Direct in-cylinder fuel injection, coupled with spark ignition, presents many vexing problems for successful engine operation. However, the potential benefits from direct injection have generated sufficient motivation for engine and fuel system designers to consider numerous fuel injection strategies (*cf.* Refs. 1-3*) One important aspect within most of these studies involves the characterization of the fuel spray behavior. These characterizations may range from relatively straight-forward bench-type flow measurements to the more difficult in-cylinder measurements of local air/fuel ratios.

In this paper, we first describe a new measurement technology for characterizing the spatial and temporal dependence of mass flux in a transient fuel spray. Our motivation for the development of a device capable of measuring mass flux in a transient fuel spray stems from experience in studying the behavior of transient fuel sprays [4]. For example, measurements of droplet size and velocity in diesel-type fuel sprays using phase/Doppler systems can be very illuminating as to the behavior of droplets. However, large droplet number densities or liquid volume fractions make characterization of the spray behavior from phase/Doppler measurements difficult. This difficulty arises when liquid mass traverses the control volume without being measured. Therefore, characterization of spray behavior from droplet size distributions using results from the subset of measured liquid mass can be misleading. This problem is particularly evident when measuring flux quantities.

While it would be desirable to have a complete description of the liquid mass in the fuel spray at any point in space and time, it has, so far, been impossible to obtain for the complex sprays that are used in reciprocating engines. Within this study we have measured mass flux temporally and spatially because of its potential significance on the overall spray behavior.

The second portion of the paper consists of data obtained with the new characterization technique which are used to compare two injection systems. Both systems have potential for use in direct injection spark ignition combustion systems.

II. EXPERIMENTAL METHOD

To provide the temporal and spatially dependent mass flux measurements, a patternator consisting of an array of small tubes and a shutter placed above the sample tubes was developed. This device is described in detail in Ref. [5]. Only a summary of the operating principles and potential sources of error will be presented here.

Figure 1 summarizes the principle of the method by illustrating the sampling of an ideal fan spray. View 1 symbolizes the spray exiting an injector at time t as the leading edge of a shutter approaches the inlet to a sample tube array. At time $t+\Delta t$, illustrated in View 2, the isolation of a spray segment within the sample tube array is denoted. The isolated spray segment thereafter is segregated from the remainder of the injection. Note that the shutter does not interact with the

* *Numbers in brackets designate references enumerated within the Reference section*

isolated spray segment. In fact, the only interaction between the shutter and spray plume occurs after sampling has taken place.

The assumption of the shutter isolating a fan spray can be extended into three-dimensions as described in Figure 2. View 1 of Figure 2 denotes a cone shaped spray exiting an injector as the shutter approaches the sample tube array. The sample volume within the spray plume is the region within the spray plume that may potentially be sampled by the sample tube array. The thickness of the sample volume is constrained

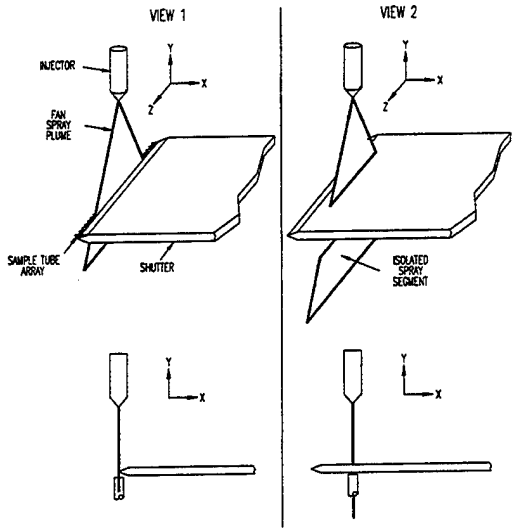

Figure 1: Schematic of the Isolation of a Fan Spray with use of a Shutter

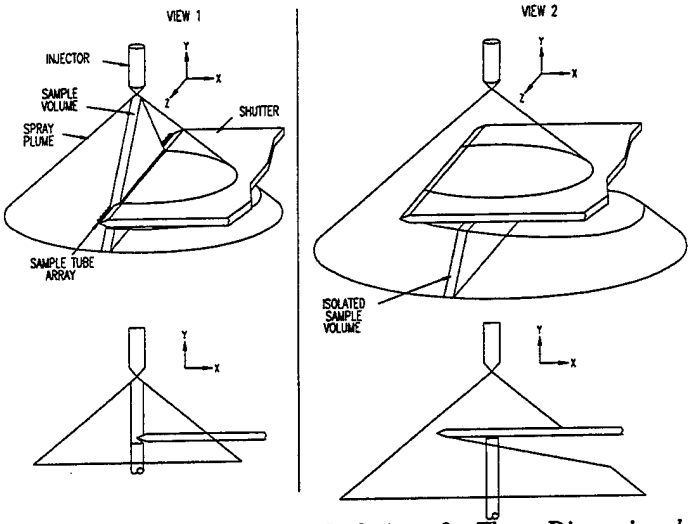

Figure 2: Schematic of the Isolation of a Three-Dimensional Spray with use of a Shutter

by the inner diameter of the sample tubes as shown in the lower image of View 1. View 1 portrays the beginning of isolation as the shutter passes through the sample volume. Within View 2, the shutter maintains segregation of the isolated sample volume for the remainder of the injection.

III. DETERMINATION OF MASS FLUX

The following section derives the relationship used to calculate the average vertical liquid mass flux at a point positioned below an injector.

A collection tube is placed at a point Y_{st} below injector and a distance z normal to the injector axis as shc in Figure 3.

The inlet of the tube samples the spray until time when the shutter isolates the sample tube inlet as shown Figure 4.

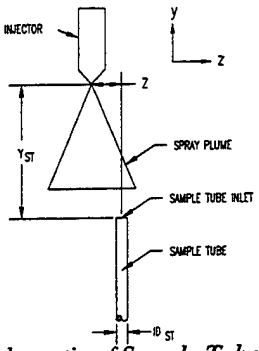

Figure 3: Schematic of Sample Tube Placement Relative to the Injector

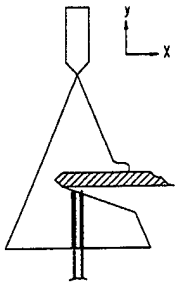

Figure 4: Schematic Cross-section of Spray Isolation at the Time of Shutter Closing t_i

The process of spray sampling and isolation at time t_i is repeated for N_i injections until an adequate volume of liquid has been captured by the sample tube inlet and passed to a customized burette. The volume of liquid is measured relative to a reference level dh_i as depicted in Figure 5. The

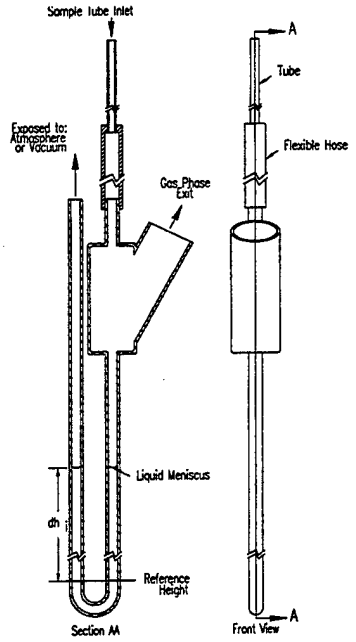

Figure 5: Total Liquid Mass Collected After Time t_i Within a Customized Burette

reference level is chosen after each collection system obtains quasi-steady state operation. For this experiment, quasi-steady state was defined as a constant rate of change of the liquid meniscus height

The average amount of mass collected per injection $\overline{M}_i$ is obtained by dividing the total liquid mass collected by the number of injections. (See Eqn. 1).

$$\overline{M}_i = \frac{dh_i \rho \pi ID_{bur}^2}{2N_i} \quad (1)$$

Where: $\overline{M}_i$ = *average liquid mass collected per injection*
dh_i = *measured change of height in burette*
ρ= *liquid density*
π=3.1415
ID_{bur}=*Inner diameter of burette*
N_i=*number of injections sampled*

The process of spray sampling is repeated for a shutter closure time after t_i referred to as t_{i+1}. The new shutter closure time, t_{i+1}, is obtained by advancing the start of injection (SOI) relative to shutter position by time step, Δt, while keeping all other variables fixed. Within this experiment, the injection was advanced 1 crank angle degree of disk (or shutter) rotation while running at 202 revolutions per minute which equates to a Δt of 0.8 msec. Applying Eqn. 1 at t_{i+1}, Eqn. (2) is obtained:

$$\overline{M}_{i+1} = \frac{dh_{i+1} \rho \pi ID_{bur}^2}{2N_{i+1}} \quad (2)$$

Where: $\overline{M}_{i+1}$ =*average liquid mass collected per injection*
dh_{i+1} =*measured change of height in burette*
N_{i+1} = *number of injections sampled*

The average vertical liquid mass flux at the point (z,Y_{st}) is obtained by dividing the difference in collected mass for events *i* and *i*+1 by the product of the time step and average sample tube area as shown in Eqn. (3).

$$\overline{M}''_{i \rightarrow i+1} = \frac{\overline{M}_{i+1} - \overline{M}_i}{(t_{i+1} - t_i) \cdot \overline{A}_{st}} \quad (3)$$

Where: $\overline{M}''_{i \rightarrow i+1}$ =Average vertical liquid mass flux
$\overline{A}_{st}$ =Average sample tube area
t_i =Shutter closure time for event i
t_{i+1} =Shutter closure time for event i+1

In addition, the difference between shutter closure times t_i and t_{i+1} is equivalent to the advancement of the injection Δt.

$$\Delta t = t_{i+1} - t_i \quad (4)$$

By combining and simplifying Eqns. (1) through (4), Eqn. (5) is obtained which is used to calculate the average vertical liquid mass flux occurring at a point (r,Y_{st}) below the injector.

$$\overline{M}''_{i \rightarrow i+1} = \frac{\rho \cdot ID_{bur}^2}{2\Delta t \cdot \overline{A}_{st}} \left\{ \frac{dh_{i+1}}{N_{i+1}} - \frac{dh_i}{N_i} \right\} \quad (5)$$

Within Eqn. (5), the term "average" is used to describe the population, spatial, and temporal averaging that occurs. The population averaging is due to the finite number of injections required to obtain measurable volumes of liquid. Spatial averaging occurs over the sample tube inner diameter while temporal averaging transpires over the time step Δt. Since the inlets of the sample tubes are positioned in a plane normal to the injector axis, the vertical component to the mass flux is captured; thus, the description of "vertical". Lastly, the term "liquid" refers to capture of only the liquid phase within the spray.

IV. EXPERIMENTAL HARDWARE

The primary hardware used within this experiment were the shutter and patternator. The shutter consisted of a rotating disk 0.6 cm thick with two symmetrical 90 degree cutouts as shown in Figure 6. A shaft encoder mounted on the shaft of the rotating disk provided the signals required to phase the SOI with the disk position.

The patternator consisted of 23 sample tubes with an OD of 0.24 cm, ID of 0.16 cm and a center to center spacing of 0.38 cm. A customized burette was placed downstream of every sample tube to allow measurement of the total sampled volume. To minimize the effects of the stagnation region at the inlet of the each of the sample tubes, a gas vent which allowed the separation of the gas and liquid phases was added to each of the burettes. Figure 5 provides a cross section of the burette used in the experiment.

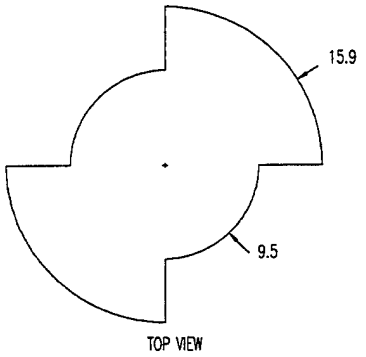

Figure 6: Top View of the Shutter Consisting of a Rotating Disk (Units: cm)

V. DATA CONSISTENCY CHECKS

Conservation of mass was applied to evaluate the effectiveness of the patternator. For axisymmetric sprays, the integral of a sampled distribution along a line normal and intersecting the spray centerline represents the liquid volume below the sample plane. If an entire plume is sampled by the patternator (no isolation with a shutter occurring), the integrated distribution should approximate the total volume injected. For comparison, the volume injected was measured independently of the patternator by the more commonplace technique of injecting into a large container and dividing the

volume collected by the number of injections. Using the ratio of the integrated volume to the measured, a collection efficiency was calculated according to Eqn. 6.

$$\eta_{col} = \frac{V_{integ}}{V_{meas}} \cdot 100 \qquad (6)$$

Where: η_{col} = collection efficiency
V_{integ} = integrated volume
V_{meas} = measured volume

For the three high-pressure single-liquid systems and one air-assisted system tested to date, collection efficiencies between 90% and 110% were typical.

Mechanisms generating disturbances within the air via the rotating disk could be categorized into three areas: shutter-induced leading edge effects, bulk fluid motion from viscous effects, bulk fluid motion from disk aerodynamics associated with disk distortion. Predictions of their effects on spray dynamics were hard to estimate. Therefore, experimental work was used to indicate the shutter's impact on the spray plume. The experimental procedure and a description of the results are outlined below.

First, the disk was locked in place with the shutter in the open position relative to the injector. The injector was pulsed until a mass distribution measurement was possible for the entire spray plume. At this point, the system was acting as a quasi-steady state patternator commonly used in spray studies [6]. Next, the disk was rotated at the speed to be used in the transient measurements and the SOI was synchronized such that the entire spray plume passes by through an open shutter condition. The distribution measured while the disk was running had to be equivalent to the quasi-steady state distribution to validate negligible bulk motion effects. Figure 7 is an illustration of possible biasing on the measured mass distribution due to an excessive disk speed. In this case, the disk speed would be reduced until the distributions obtained with the disk stationary and running were equivalent within experimental uncertainty. For the injection systems used in this experiment, disk speeds of less than 300 revolutions per minute were required to meet this criteria.

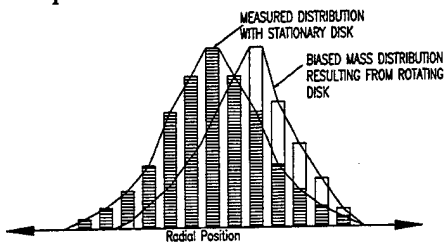

Figure 7: Schematic Demonstrating Biasing by Shutter Effects

Experimental uncertainty in the mass flux calculations was estimated using a method proposed by Kline and McClintock [7]. This method was applied to Eqn. 5 to estimate a maximum uncertainty of ±1 g/cm^2/sec for the high pressure atomizer and ±0.6 g/cm^2/sec for the air assist system. Resolution limitations of the burettes at ±1 mm was the primary source of error in the estimate. However, by increasing the number of injections sampled (N), the uncertainty decreases as observed in the air assist error.

VI. EXPERIMENTAL CONDITIONS

Within this study, the average volume of fuel per injection was 69 mm^3. For most SI engine applications, this represents a large quantity of fuel. However, this operating point was chosen to provide comparable pulsewidths and delivery rates for both systems. For comparison, a smaller volume of 20 mm^3 is provided in the mass flux contour results for the pressure atomizer.

Both images and mass flux data were collected in ambient room conditions. Stoddard solvent was used instead of gasoline throughout the study. Spray images were captured with a CID camera illuminated with a 50 µsec strobe from the left side. Black and white within the images were transposed for improved clarity.

The air-assist atomizer consisted of on outward opening poppet held in place by a spring in compression. An injection cycle began with the opening of a fuel solenoid which charged a cavity with the desired volume of fuel. The pulsewidth of the fuel solenoid dictated fuel volume. The fuel solenoid closed prior to opening of the air solenoid. After fuel solenoid closure, an air solenoid opened charging the cavity with air until the poppet was forced open. Due to the spring tension and the poppet interaction with the cavity pressure and fluid forces, the poppet oscillated throughout the injection. The end of injection occurred after air solenoid closure and the subsequent cavity blowdown. Additional information on the injector can be found in papers by Schechter and Levin [8], Felton and Bracco [9].

The pressure atomizer used in the study consisted of an inwardly opening pintle. Control of the solenoid that controls pintle position dictated the injection duration and subsequent volume injected.

The operating conditions used in the study are provided in Table 2.

Table 2: Operating Conditions

Injector	Fuel Delivery (mm^3/inj)	Air PW (msec)	Fuel PW (msec)	Fuel Press. (kPa)	Air Press (kPa)
Air-assist	69.0	4.7	26.0	276	689
Pressure Atomizer	69.0	na	4.0	6895	na
Pressure Atomizer	20.0	na	1.1	6895	na

na: not applicable

VII. RESULTS

Figure 8 is a plot of the volumetric delivery of liquid fuel passing through a plane 1 cm below the injector as a function of time. The distance of 1 cm was the clearance necessary to accommodate the rotating disk. The data within Figure 8 were generated by isolating the spray at various times after the start of injection. Start of injection throughout this study is defined as the moment when the pintle or poppet begins to unseat. The distribution measured by the patternator

was integrated about the injector axis to obtain an estimate of the volume of liquid below the 1 cm plane.

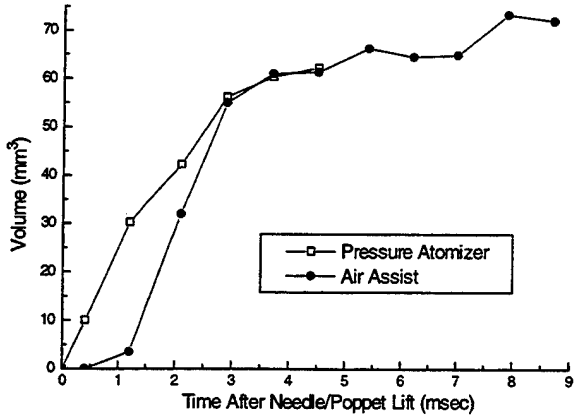

Figure 8: Time Versus of Liquid Fuel Passing Through a Plane 1 cm Below the Injector

Fuel delivery of the pressure atomizer was linear over the pulsewidth, with the exception of the last two milliseconds as shown in Figure 8. At the time of pintle closure, the integrated volume estimated from the transient patternator results was 62 mm^3 in comparison to the measured average volume of 69 mm^3. This was most likely error associated with uncertainty within the patternator measurements.

The air-assist data suggests that volume flux lags behind initial poppet movement by as much as 1.25 msec. Once the flow is initiated, a surge occurred delivering 60 mm^3 or 87% of the total delivery over a 3.0 msec period. Figure 9 provides a trace of the poppet lift as a function of time in conjunction with the air-assist volume versus time data. It appears that the high volume flux coincided with the first poppet bounce. The two bounces that follow contribute only 10 mm^3 of the remaining injection. Error associated with uncertainty within the patternator measurements contribute to the overestimate of 73 mm^3, which is 4 mm^3 higher than the measured 69 mm^3. The same sources of error also contribute to the small dips in flux that exist at 6.26 msec and 8.75 msec.

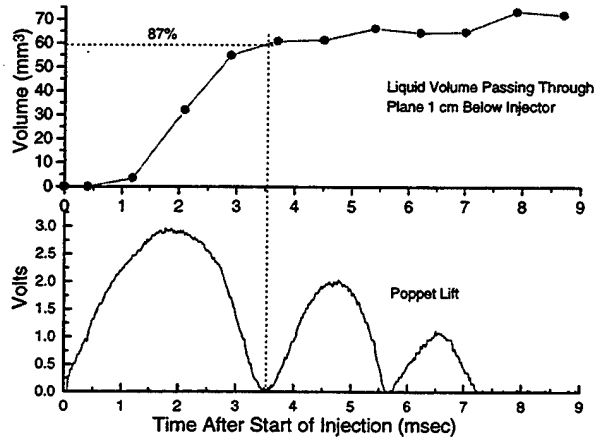

Figure 9: Poppet Lift and Volume Versus Time for the Air-Assist Atomizer

Comparisons of the mass flux occurring at a plane 1 cm below the injector for various time steps beginning at SOI are shown in Figure 10. The distance between sample points or resolution was 0.19 cm.

Mass flux data suggests that both systems provided a symmetrical hollow distribution about the injector axis. (Data obtained by raising and rotating the injectors suggests that this is the case throughout the plumes for both systems).

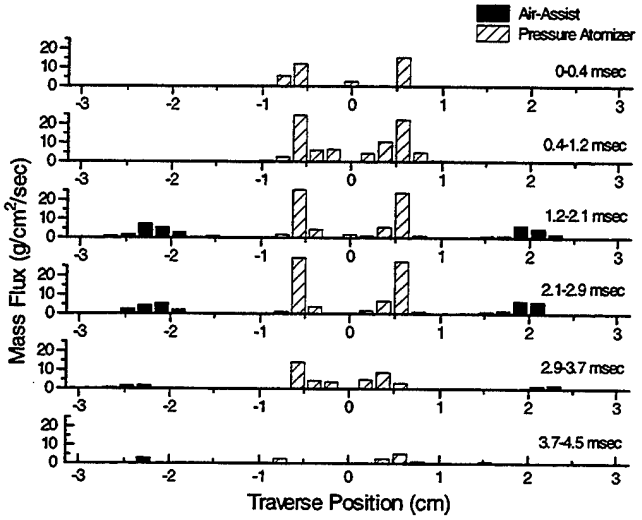

Figure 10: Mass Flux occurring at a Plane 1 cm Below the Injector for the Pressure Atomizer and Air Assist (Vol/Inj.=69 mm^3)

The air-assist data exhibited a wide hollow distribution. Initial mass flux was low due to the lag noted in Figure 8. Beginning with the time period of 1.2-2.1 msec a maximum mass flux of 7 g/cm^2/sec was measured which then decreased for the remainder of the injection.

In contrast, the pressure atomizer exhibits a narrow hollow cone distribution. Within the time period of 0.4-2.9 msec, the maximum measured mass flux was approximately 25 g/cm^2/sec.

Figures 11 through 13 consist of both mass flux contour plots and spray images captured by a CID camera. The spray images are positioned towards the top of the figure with the capture time after SOI noted below the image. The spray images positioned to the upper left and right of each contour plot represent the beginning and end of the sampling period depicted by the corresponding contour plot. The contour plots positioned towards the bottom of the figure were generated by linearly interpolating mass flux data at a series of distances below the injector. The contours depict mass flux occurring below the injector for the time period shown at the bottom of each plot. Due to the linear interpolation schemes combined with limited resolution, the mass flux contours may at times exhibit sharp angles not expected in the data. Both spray images and contours are scaled to 50% of their actual size.

Spray development of the plume generated by the pressure atomizer for the injected quantity of 69 mm^3 is shown in Figure 11. To decrease data collection times, a lower resolution of 0.38 cm was used between sample tubes. Consequently, high mass flux gradients within Figures 11 and 12 do not correlate well with Figure 10 where gradients were measured more precisely with a resolution of 0.19 cm. For the

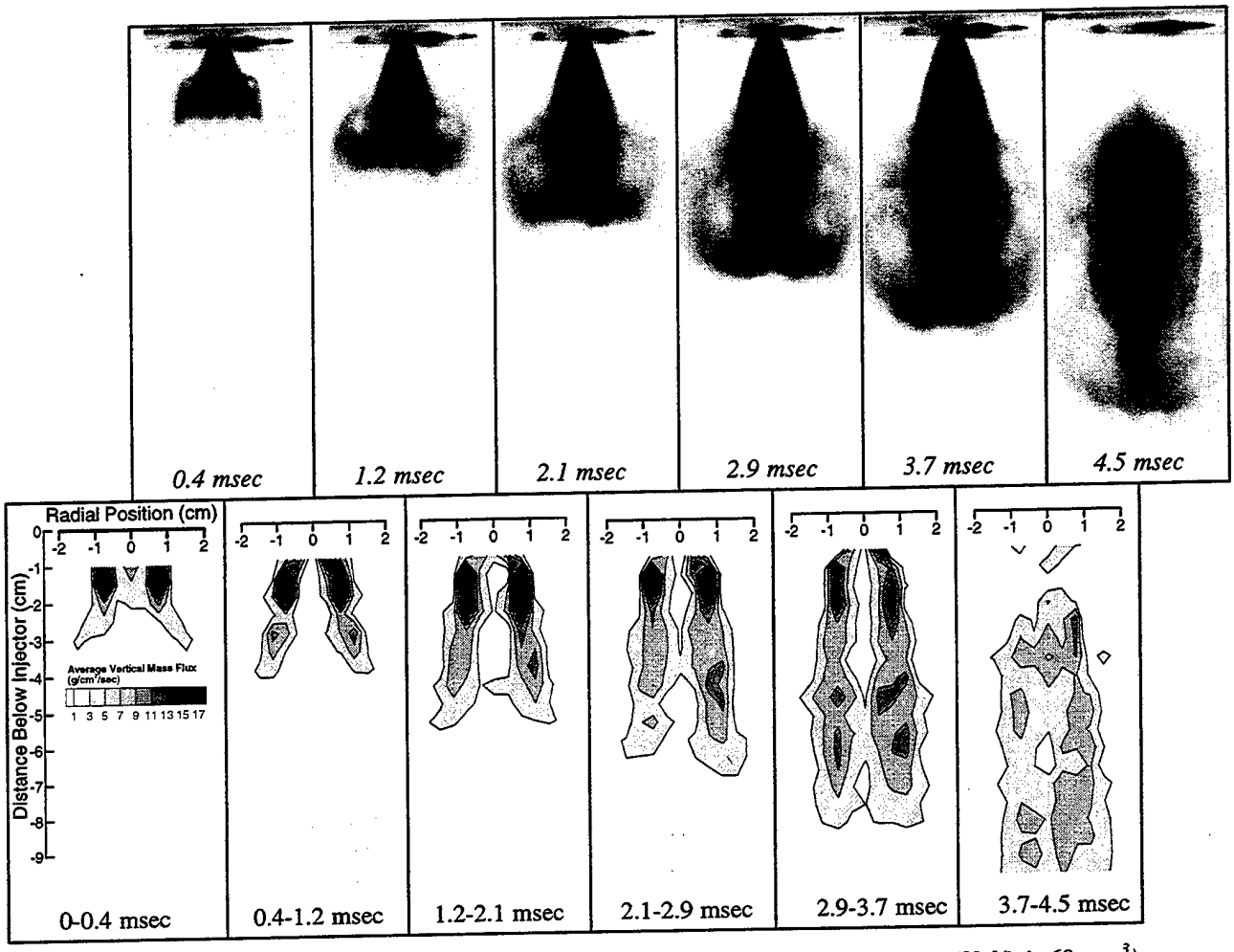

Figure 11: Spray Images and Mass Flux Contours for the High Pressure Atomizer (Vol/inj=69 mm^3)

time period of 0-0.4 msec, mass flux was primarily located in the outer edges with a small amount of flux measured along the centerline. For the time period of 0.4-1.2 msec, the spray has developed into a hollow cone structure. Indentations in the outer plume wall at 2.5 cm below the injector occur in the region where vortices interact with the outer spray sheet. This phenomena has been noted in a previous study of an entirely different pressure atomizer [10]. Below the indentation, the magnitude of the measured mass flux decreases with the widening of both the cone angle and wall thickness. This thickening of the outer walls becomes more pronounced in mass flux contours for next period of 1.2-2.1 msec. In addition to widening of the walls, mass flux measured along the centerline at 4.5 cm below the injector hints to the eventual collapse of the hollow cone region into a cylindrical structure as shown in the time period of 2.1-2.9 msec. Note that the collapsing shown for the time period of 2.1-2.9 msec occurs below the top reentry point of the vortex, at 2.5 cm below the injector. For the time period of 2.9-3.7 msec, the spray walls continue to thicken along with additional collapsing along the centerline. The effects of the pintle closure are observed as a decrease in mass flux measured close to the injector. The final time period of 3.7-4.5 msec demonstrates a dispersed cylindrical spray plume with few signs of its hollow cone origins.

Additional data from the pressure atomizer for a low delivery of 20 mm^3 is provided in Figure 12. The first contour

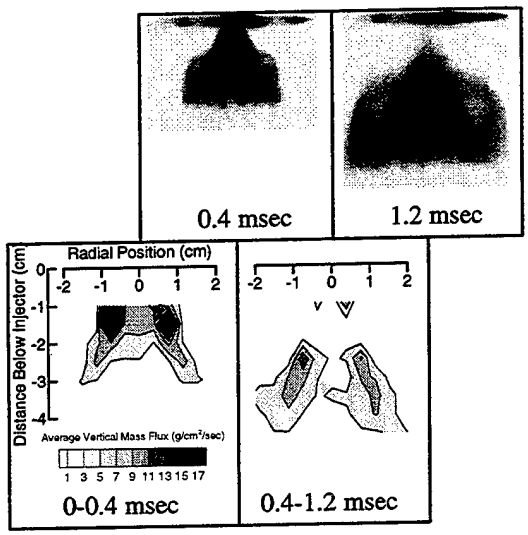

Figure 12: Spray Images and Mass Flux Contours for the High Pressure Atomizer (Vol/inj=20 mm^3)

plot representing the time period of 0-0.4 msec is similar to the same period for the 69 mm^3 case. Any differences between the two images are attributed to uncertainty of the patternator measurements. The contour plot for the time period of 0.4-1.2 msec demonstrates a hollow cone structure with dispersed walls.

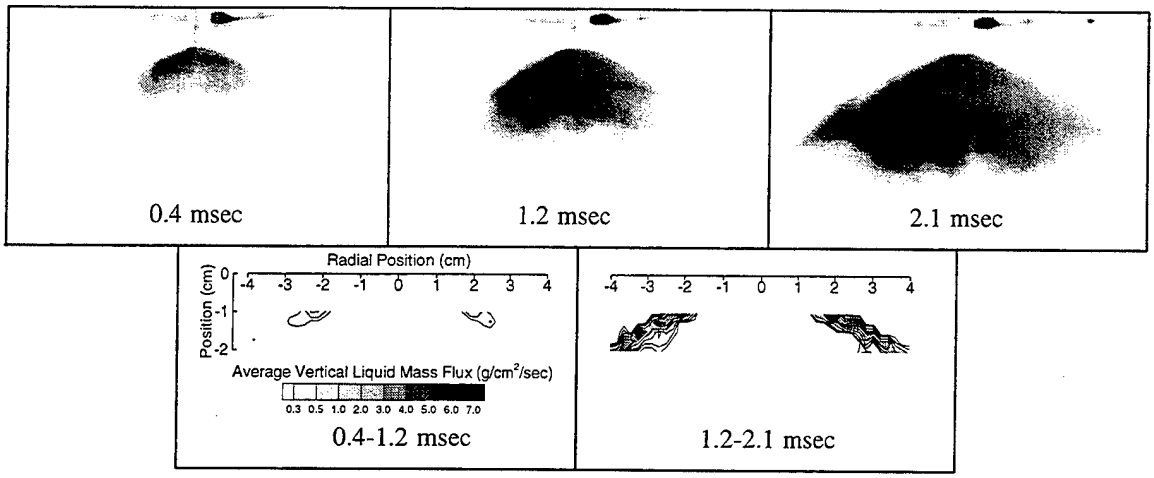

Figure 13:Spray images and Mass Flux Contours for the Air-Assist Atomizer (Vol/inj=69 mm^3)

The air-assist case with an injection quantity of 69 mm^3 is represented in Figure 13. Mass flux contours were not generated prior to 0.4 msec or past 2.9 msec due to the fact that small amounts of mass were injected prior to or after that time as discussed earlier. Both contours maintain a hollow cone structure for the region shown (1 to 2 cm below the injector). Mass flux measurements were not taken below 2 cm due to width limitations of the patternator. There is some evidence of collapse lower than 2 cm but a majority of the mass flux remains outside a 4 cm radius from the injector centerline.

VIII. SUMMARY

This study investigated two distinct atomization strategies: pressure atomization and air-assist via mass flux measurements on a spatial and temporal basis. The method used to obtain the mass flux measurements was a new development incorporating a patternator designed to minimize stagnation effects and a concept of isolating the spray with a shutter. Due to the obtrusive nature of this mass flux measurement, methods used to check data consistency were discussed.

Mass flux data suggested that the air-assist system operating with a fuel delivery of 69 mm^3 expelled up to 87% of its delivery within a 3.0 msec period even though the poppet oscillated for a total of 7.25 msec. The timing of the 3.0 msec surge suggests it occurred during the first of three poppet lifts. The air-assist system also exhibited a wide hollow cone structure for the limited region where mass flux measurements were made.

The pressure atomizer provided a linear delivery over a majority of the pulsewidth. Mass flux data revealed that initially, mass was distributed in the outer walls of the plume but eventually collapses into a dispersed cylindrical structure. Mass flux data also suggested that interaction with the reintrainment vortex may have contributed to the internal widening of the spray walls and eventual collapse. Lastly, with a delivery of 20 mm^3, mass flux contours for the pressure atomizer resembled the higher flow rate for the first time step. However, the second and last time step revealed a hollow cone structure with thick dispersed walls.

ACKNOWLEDGMENTS

Funding for this work was generously provided by the Wisconsin Small Engine Consortium (WSEC) and the department of Administration of the State of Wisconsin. The Engine Research Center is also supported by the Army Research Office through grant Nos. DAAH04-94-G-0328 and DAAHL03-92-0122. The authors acknowledge Mercury Marine, Division of Brunswick Corp. for the fabrication of the hardware used within this experiment and Scott Parrish for his assistance and suggestions with the spray images.

REFERENCES

1. Syvertsen, Marc L., et. al., "*Injection and Ignition Effects on Two-Stroke Direct-Injection Emissions and Efficiency*", SAE Paper No. 961803, Society of Automotive Engineers, Warrendale, PA, 1996.

2. Ghandhi, Jaal B., and F.V. Bracco, "*Fuel Distribution Effects on the Combustion of a Direct-Injection Stratified-Charged Engine*", SAE Technical Paper Series, SAE Paper No. 950460, Society of Automotive Engineers, Warrendale, PA, 1995.

3. Fansler, Todd D., D.T. French, and M.C. Drake, "*Fuel Distributions in a Firing Direct-Injection Spark-Ignition Engine using Laser-Induced Fluorescence Imaging*", SAE Paper No. 950110, Society of Automotive Engineers, Warrendale, PA, 1995.

4. Koo, Ja-Ye, and J.K. Martin, "*Droplet Sizes and Velocities in a Transient Diesel Fuel Spray*", SAE Paper No. 900397, Society of Automotive Engineers, Warrendale, PA, 1990.

5. Hoffman, Jeffrey A., Jay K. Martin, and Sam W. Coates, "*Spatial and Temporal Mass Flux Measurements of a Pulsed Spray - a Review of the Hardware and Methodology*", Submitted to the Review of Scientific Instruments- February, 1997.

6. Parrish, Scott, and Larry Evers, "*Spray Characteristics of Compound Silicon Micro Machined Port Fuel Injector*

Orifices", SAE Paper No. 950510, Society of Automotive Engineers, Warrendale, PA, 1995.

7. Kline, S. J., and F. A. McClintock, "Describing Uncertainties in Single-Sample Experiments", Mechanical Engineering, January, 1953.

8. Schechter, Michael M., and Michael B. Levin, "*Air-Forced Fuel Injection System for 2-Stroke D.I. Gasoline Engine*", SAE Paper No. 900478, Society of Automotive Engineers, Warrendale, PA, 1990.

9. Emerson, J., P.G. Felton, and F.V. Bracco, "*Structure of Sprays from Fuel Injectors Part III: The Ford Air-Assisted Fuel Injector*", SAE Paper No. 900478, Society of Automotive Engineers, Warrendale, PA. 1990.

10. Hoffman, Jeffrey A., Jay K. Martin, and Sam W. Coates, "*Spray Photographs and Preliminary Spray Mass Flux Distribution Measurements of a Pulsed Pressure Atomizer*", ILASS-Americas 96, 9th Annual Conference of Liquid Atomization and Spray System, San Francisco, 1996.